

# How did the ecological civilization policy rebuild the Human-Water Relationships in the 600-year old “Tunpu” area, China?

Yang Shengtian<sup>1</sup>, Pan Zihao<sup>2</sup>, Lou Hezhen<sup>2</sup>, Li Chaojun<sup>2</sup>, Zhang Jun<sup>3</sup>, Zhang Yujia<sup>1</sup>, Yi Yin<sup>4</sup>, Gong Jiyi<sup>4</sup>, Luo Ya<sup>5</sup>, and Li Xi<sup>4</sup>

<sup>1</sup>Beijing Normal University

<sup>2</sup>beijing normal university

<sup>3</sup>College of Water Sciences

<sup>4</sup>guizhou normal university

<sup>5</sup>Unknown

November 16, 2022

## Abstract

With the intensification of climate change and population growth, human-water relationships (HWR) have changed from the simple utilization of water resources to changing the spatial distributions and distribution proportions of water resources through formulating corresponding policies, such as Chinese ecological civilization policy. However, the impact of the ecological civilization policy on the evolution of HWR is still unclear. Here, taking the 600-year old “Tunpu” area as a typical study area, this research analyses the evolution of HWR over different space and time spans based on the Remote Sensing Hydrological Station (RSHS) technology, an improved water balance formula and the transition theory. The results show that at the village scale, the water cycle structure of a typical village has remained stable, and deforestation has increased the proportion of runoff to precipitation by 10.62%. At the basin scale, due to land use/cover changes and precipitation fluctuations, the trend of the runoff changes from slowly decreasing to accelerated increases, with change rate increasing from  $-0.073 \times 10^4 \text{ m}^3 \cdot \text{a}^{-1}$  in the Ming Dynasty (1470-1636) to  $30.946 \times 10^4 \text{ m}^3 \cdot \text{a}^{-1}$  in the China stage (1949-2020). HWR have developed from the initial balanced resource-rich period to the unbalanced extensive-development period and have finally changed into a rebalancing period under the influence of the ecological civilization policy. Four stages of HWR are as follows: predevelopment (1470-1685), take off (1685-1912), acceleration (1912-2000) and rebalancing (2000-2020). This research indicates that the ecological civilization policy can rebuild HWR, and it is expected to provide enlightenment for future construction of the ecological civilization.

---

# How did the ecological civilization policy rebuild the Human-Water Relationships in the 600-year old “Tunpu” area, China?

Shengtian Yang<sup>1</sup>, Zihao Pan<sup>1</sup>, Hezhen Lou<sup>1,\*</sup>, Chaojun Li<sup>1</sup>,

Jun Zhang<sup>1</sup>, Yujia Zhang<sup>1</sup>, Yin Yi<sup>2</sup>, Jiyi Gong<sup>2</sup>, Ya Luo<sup>3</sup>, Xi Li<sup>3</sup>

(1. College of Water Science, Beijing Normal University, Beijing 100875, China;

2. School of Life Sciences, Guizhou Normal University, Guiyang, Guizhou, 550025, China;

3. School of Geographic and Environmental Sciences, Guizhou Normal University, Guiyang 550025, China)

\*Correspondence to: Hezhen Lou (11112019051@bnu.edu.cn)

**Abstract:** With the intensification of climate change and population growth, human-water relationships (HWR) have changed from the simple utilization of water resources to changing the spatial distributions and distribution proportions of water resources through formulating corresponding policies, such as Chinese ecological civilization policy. However, the impact of the ecological civilization policy on the evolution of HWR is still unclear. Here, taking the 600-year old “Tunpu” area as a typical study area, this research analyses the evolution of HWR over different space and time spans based on the Remote Sensing Hydrological Station (RSHS) technology, an improved water balance formula and the transition theory. The results show that at the village scale, the water cycle structure of a typical village has remained stable, and deforestation has increased the proportion of runoff to precipitation by 10.62%. At the basin scale, due to land use/cover changes and precipitation fluctuations, the trend of the runoff changes from slowly decreasing to accelerated increases, with change rate increasing from  $-0.073 \times 10^4 \text{ m}^3 \cdot \text{a}^{-1}$  in the Ming Dynasty (1470-1636) to  $30.946 \times 10^4 \text{ m}^3 \cdot \text{a}^{-1}$  in the China stage (1949-2020). HWR have developed from the initial balanced resource-rich period to the unbalanced extensive-development period and have finally changed into a rebalancing period under the influence of the ecological civilization policy. Four stages of HWR are as follows: predevelopment (1470-1685), take off (1685-1912), acceleration (1912-2000) and rebalancing (2000-2020). This research indicates that the ecological civilization policy can rebuild HWR, and it is expected to provide enlightenment for future construction of the ecological civilization.

**Keywords:** Socio-hydrology; Human-Water Relationships; Reconstruction of water cycle; Remote sensing; Ecological civilization.

## 1 Introduction

Human-water relationships (HWR) have changed from the simple utilization of water resources to changing the spatial distributions and distribution proportions of water resources through formulating corresponding policies because of the

---

29 intensification of climate change and population growth (Li et al., 2020). For example, to change the relationship between  
30 China's existing development model and the ecological environment, the Chinese government officially put forward the  
31 “ecological civilization” policy in 2007 (Hansen et al., 2018; Zhang et al., 2018). To date, the ecological civilization has  
32 become the basic ideological framework for China to develop stricter environmental policies (Zhang et al., 2018) and has had  
33 a significant impact on China's society, citizens and national policies (Pan, 2012; Xiao and Zhao, 2017; Sha and Iop, 2018;  
34 Lu et al., 2019). Due to the important role of water in ecosystem stability and supporting human development (Falkenmark,  
35 2001; Ceola et al., 2016), the “water ecological civilization” has always been an important part of the ecological civilization  
36 society (Li et al., 2020). Its purpose is to solve the shortage of water resources, deterioration of the water environment and  
37 other water problems that are caused by socioeconomic development, so as to make human and water systems develop  
38 harmoniously, which lead to the construction of the ecological civilization that will inevitably affect HWR (Liu and Wang,  
39 2018; Tian et al., 2021). However, most of the studies on the water ecological civilization focus on constructing an evaluation  
40 index system, and most of the indicators mainly consist of changes in water systems (Li et al., 2020; Tian et al., 2021; Q. Yang  
41 et al., 2021). The impact of major ecological policies, e.g., the ecological civilization, on the evolution of HWR is still unclear.

42       Currently, studies on the evolution of HWR (Ahmad et al., 2018; Bao and Zou, 2018; Zhao et al., 2020; Zuo et al., 2020;  
43 Zuo et al., 2021) are abundant, especially for those countries and areas with a long history of water resource development.  
44 The great changes in the natural and social environments will significantly affect the evolution of HWR, which can help us  
45 to understand the processes of water problems and are of great significance for improving the understanding of HWR in the  
46 past and accurately predicting their possible future dynamics (Sivapalan et al., 2012; Liu et al., 2014; Liu et al., 2015).  
47 Therefore, to overcome the limitations of studies with short-time spans that rely on detailed statistical data, some scholars  
48 have used the historical literature and hydrological methods to study the evolution of HWR over a span of more than one  
49 thousand years in the Tarim River Basin (Liu et al., 2014), Heihe River Basin (Lu et al., 2015), Loess Plateau of China (Wu  
50 et al., 2020) and whole China (Wang et al., 2017). The above studies that analyse the evolution of HWR over long periods  
51 mainly express the changes in water systems in HWR by using indicators such as temperature, dry and wet climate or  
52 precipitation. In addition, runoff is also an important part of the water cycle process, and its amounts are affected by many  
53 factors, such as precipitation, temperature and land use/cover change (LUCC), which more directly reflect the evolution of  
54 HWR. Due to the difficulty of obtaining runoff data from historical periods, there are few studies on the evolution of HWR  
55 over long periods from the perspective of runoff or water cycle processes (Lu et al., 2015).

56       Many areas of the world have realized the utilization of water resources and live in human-water harmony as early as  
57 thousands of years ago. For example, in 793 AD, Charlemagne the Great of the Frankish Kingdom decided to connect the  
58 Rhine/Main catchment and Danube catchment by constructing a canal known as the Fossa Carolina, and it could be used for

---

59 navigation, irrigation, flood diversion, drainage and water supplies (Leitholdt et al., 2012). In the middle reach of the  
60 Mingjiang River in Sichuan Province, China, the Dujiang Dam was initiated during the Qin Dynasty in 256 BC and has been  
61 playing the roles of flood control and irrigation for more than 2000 years (Li and Xu, 2006). Besides, there is such a “Tunpu”  
62 area in China's experimental ecological civilization area, Guizhou Province, which has its own unique culture and a  
63 600-year history of water resources development, which makes the “Tunpu” area suitable for studying the evolution of HWR  
64 over long periods. In 1902, the Japanese scholar, Torii Ryuzo, first discovered the “Tunpu” area and found that as far back as  
65 600 years ago, the “Tunpu” area was inhabited by immigrants who were of Han nationality rather than of Miao nationality,  
66 who formed a precious and characteristic “Tunpu” culture (Nie, 2017). Due to the advanced farming technology and ability  
67 to build water conservation projects of the Han nationality immigrants, the “Tunpu” people could make full and efficient use  
68 of their water resources, which included irrigating paddy fields at different altitudes, effectively resisting drought and flood  
69 discharges, and providing domestic water and hydropower for the entire village (Zhang and Pang, 2007).

70 Therefore, taking the “Tunpu” area as a typical study area, based on the Remote Sensing Hydrological Station (RSHS)  
71 technology and an improved water balance formula, we tried to find significant implications from the HWR in this famous  
72 area, the main study contents of this research include the following three points: (1) The historical and modern water cycle  
73 processes at the village scale are reconstructed; (2) Then 600 years' LUCC was also retrieved by using remote sensing and  
74 historical data, and the water cycle processes at the basin scale are reconstructed over the past 600 years. (3) Based on  
75 transition theory, the key time nodes of the evolution of HWR are determined, and the impact of the ecological civilization  
76 on HWR is analysed.

## 77 **2 Study area**

78 The “Tunpu” area, with a 600-year history of water resource development, is located in Anshun city, Guizhou Province,  
79 which is an experimental ecological civilization area in China (105.975°E - 106.366°E, 26.159°N - 26.463°N). The “Tunpu”  
80 area is mainly located in the Yangchang River Basin, which belongs to the Wujiang River System in the Yangtze River Basin,  
81 with a drainage area of 721.78 km<sup>2</sup>. The basin has a north subtropical monsoon humid climate, with an annual average  
82 temperature of 14-15°C and annual precipitation of 1200-1300 mm. The presence of karst development, poor water holding  
83 capacity and high surface water permeability in the basin cause it to be prone to soil erosion and rocky desertification (Fig.  
84 1a).

85 In view of the history of water resource development and utilization and the modern ecological civilization policies in  
86 the “Tunpu” area, it is suitable for studying the evolution process of HWR over a long period. As early as 1382, the “Tunpu”  
87 area was inhabited by many Han immigrants who came from the south part of the Yangtze River and from the Central Plains,  
88 who were clearly different from the surrounding ethnic minorities and Han nationalities in their clothing, language,

architecture, customs and culture, forming a precious and characteristic “Tunpu” culture (Fig. 1a). Moreover, through the construction of water conservancy projects such as backwater weirs, “fish mouth water diversion”, water-powered rollers and water mills in “Baojia Tun” (Fig. 1b and Fig. 1c), the “Tunpu” people were able to achieve the efficient utilization of water resources and live in human-water harmony as far back as 600 years ago. In modern times, when facing the severe situation of tight resource constraints, serious environmental pollution and ecosystem degradation that were caused by accelerated socioeconomic development, Guizhou Province, where the “Tunpu” area is located, the area has actively responded to the call of the state and has implemented the construction of the ecological civilization. After 2000, key projects for the prevention and control of soil erosion were launched, and ecological construction projects focusing on returning farmlands to forests were vigorously promoted. After 2005, this area took the lead in making the strategic decision of building the ecological civilization and was established as a national ecological civilization experimental area (Jiang et al., 2014).

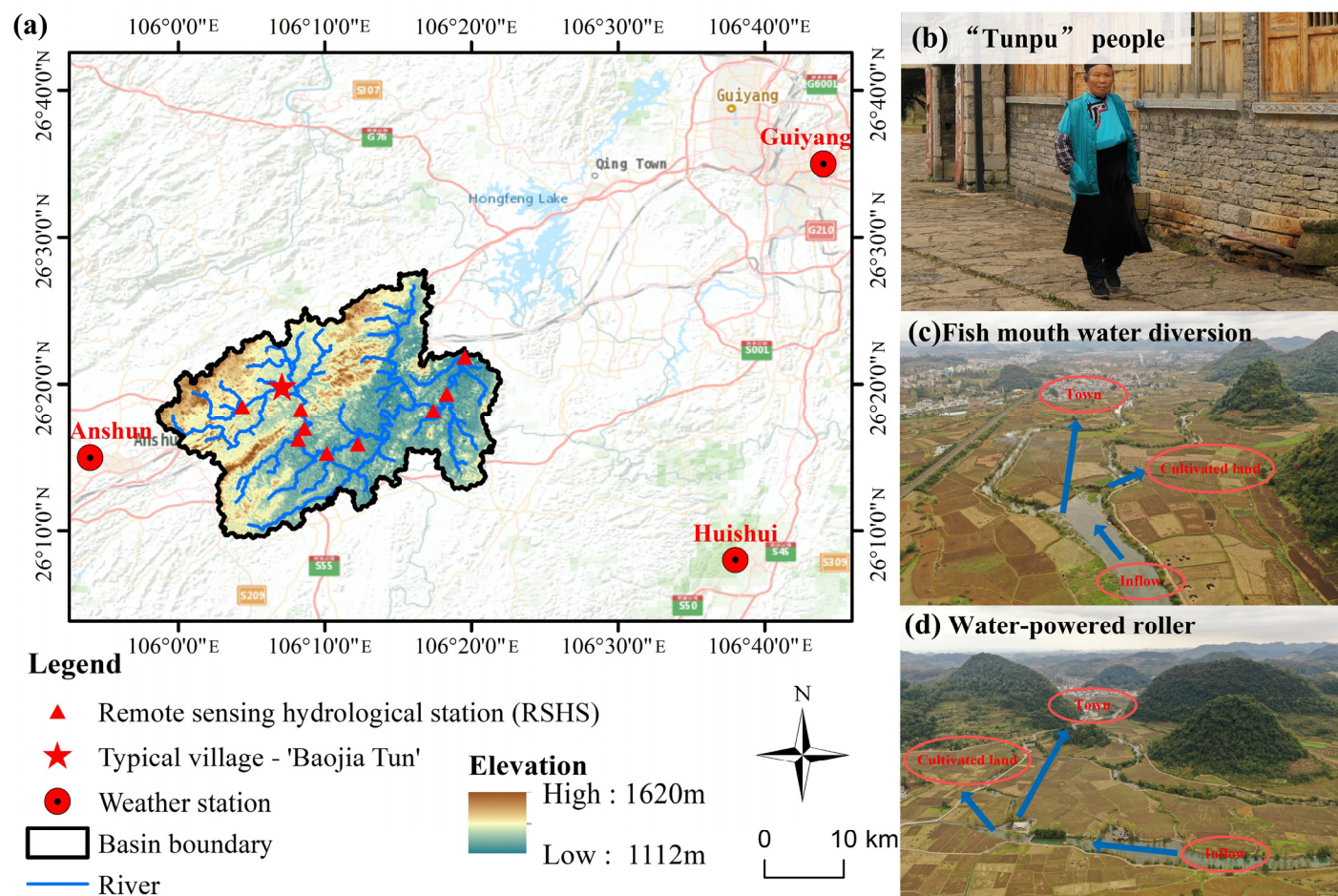


**Figure 1.** (a) Study area of this research; (b) the “Tunpu” people wear traditional costumes; (c) “Fish mouth water diversion” of “Baojia Tun”; and (d) water powered roller of “Baojia Tun”.

### 3 Methods and data

#### (1) Reconstruction of the water cycle process at the village scale

104 An improved water balance formula that considers irrigation water and domestic water is constructed. The formulas are  
 105 as follows:

$$106 \begin{cases} P - ET - \Delta W - DW = R \\ I - \Delta ET_{paddy} = IB \end{cases} \quad (1)$$

107 where  $P$  is precipitation,  $m^3$ ;  $ET$  is the actual evapotranspiration,  $m^3$ ;  $\Delta W$  is the water storage variable of the basin, which can  
 108 be regarded as 0;  $DW$  refers to the total domestic water consumption,  $100 \text{ L} \cdot (\text{capita} \cdot \text{day})^{-1}$ ;  $R$  is the total runoff,  $m^3$ ;  $I$  and  $IB$   
 109 are the irrigation water and irrigation backwater amounts,  $m^3$ , respectively, and  $\Delta ET_{paddy}$  is the difference between  
 110 evapotranspiration with irrigation and that without irrigation,  $m^3$ .

111 To analyse the changes in the water cycle structure and its elements and by assuming that the precipitation is 100%, it is  
 112 only necessary to reconstruct the evapotranspiration sequence according to the land use/cover data of the two periods, and the  
 113 changes in runoff can then be obtained. To calculate the evapotranspiration, the formula for calculating the actual  
 114 evapotranspiration is based on the Budyko hypothesis that was proposed by Fu (1981). In addition, cultivated lands are divided  
 115 into paddy fields and dry lands, and the water sources for the evapotranspiration from paddy fields include not only  
 116 precipitation but also irrigation water. The formulas are as follows:

$$117 \frac{ET}{P} = 1 + \frac{ET_0}{P} - [1 + (\frac{ET_0}{P})^w]^{1/w} \quad (2)$$

$$118 P_{paddy} = P + I \quad (3)$$

119 where  $ET_0$  is the potential evapotranspiration,  $m^3$ ;  $w$  is the basin-scale model parameter; and  $w$  was defined as 3.5 for all  
 120 land use/cover types in the arid basin, which is not applicable to the study of humid basins. Therefore, the values of  $w$  for  
 121 forestland, cultivated land, grassland and construction land are defined as 2.25, 1.7, 1.55 and 1.35, respectively;  $P_{paddy}$  is  
 122 the quantity of water resources that can be used for evapotranspiration in paddy fields,  $m^3$ ;  $I$  is the irrigation water amount,  
 123 and the irrigation quota is  $795 \text{ mm} \cdot \text{a}^{-1}$ .

## 124 (2) Reconstruction of the water cycle process at the basin scale

125 The water balance formula of reconstructing basin scale water cycle process is basically the same as that of village scale,  
 126 and the measured surface runoff data can be used to analyse the reliability of the runoff calculated by water balance formula.  
 127 Due to the small size of the basin and lack of continuous hydrological observation data, the RSHS technology can used to  
 128 address the difficulty of obtaining surface runoff data in ungauged basins (Yang et al., 2019; Zhao et al., 2019; Lou et al.,  
 129 2020; Wang et al., 2020; Yang et al., 2020; Wufu et al., 2021; S. Yang et al., 2021). The RSHS method uses an unmanned  
 130 aerial vehicle to assist the field survey in generating a digital river model with terrain data accuracies as small as the centimetre  
 131 level. Then, the long-time series of the river width data can be inverted according to satellite remote sensing Normalized  
 132 Difference Water Index (NDWI) data and the sub-pixel decomposition method (formula 4). Finally, based on the  
 133 Manning formula, the long-time series of the surface runoff data can be estimated by calculating hydraulic parameters such

as overflow area, hydraulic radius and wetted perimeter length to a specific river width (formula 5).

$$W = \sum_{i=1}^x \begin{cases} \frac{PA}{VL} & NDWI^i > NDWI_{WT} \\ \left( \frac{NDWI^i - NDWI_{LT}}{NDWI_{WT} - NDWI_{LT}} \right) * \frac{PA}{VL} & NDWI_{LT} < NDWI^i < NDWI_{WT} \\ 0 & NDWI^i < NDWI_{LT} \end{cases} \quad (4)$$

$$\begin{cases} R'(W) = V \times A = \frac{k}{n} \times HR^{2/3} \times J^{1/2} \times A \\ HR = L/A \end{cases} \quad (5)$$

where  $W$  is the average river width of the selected river valley, m;  $x$  is the total number of pixels in the selected river valley;  $NDWI^i$  is the  $NDWI$  of pixel  $i$ ;  $NDWI_{LT}$  and  $NDWI_{WT}$  are the  $NDWI$  threshold of land and water, respectively;  $PA$  is the area of each pixel,  $m^2$ ;  $VL$  is the length of the selected river valley, m;  $R'(W)$  is the estimated runoff corresponding to river width  $W$ ,  $m^3$ ;  $V$  is the flow velocity,  $m \cdot s^{-1}$ ;  $k$  is the conversion constant,  $k = 1$ ;  $n$  is the roughness, which comprehensively reflects the impacts of the river channel roughness on river flow,  $n = 0.035$ ;  $HR$  is the hydraulic radius, m;  $J$  is the slope, measured by UAV remote sensing image;  $L$  is the Wetted perimeter length, m;  $A$  is the overflow area,  $m^2$ ;  $L$  is the wetted perimeter length, m;  $HR$ ,  $L$ , and  $A$  are calculated by river width and digital river model.

However, different from the reconstruction of the water cycle process at the village scale, it is necessary to consider climate change and reconstruct the precipitation sequence year by year at the basin scale. *The atlas of drought and flood distribution in China in the past 500 years* systematically reproduces the general characteristics of the annual drought and flood distributions for the 531 years from 1470-2000 (Institute of Meteorological Sciences, 1981; Zhang and liu, 1993; Zhang et al., 2003), and the rationality of this atlas is shown by its application in the Heihe River Basin and other regions (Ren et al., 2010; Lu et al., 2015). After determining the drought and flood levels in the basin from 1470 to 2000 by using the atlas, the precipitation levels for the basin area according to the measured precipitation data of the national meteorological stations from 1959 to 2000 are calculated, and the annual precipitation anomaly percentages that correspond to each drought and flood level within an appropriate range are then determined (Table 1). In addition, the intensity of the East Asian monsoon is one of the main factors that affects the precipitation in the basin, and the study area also experienced a small ice age (1470-1633), strong monsoon period (1634-1950) and weak monsoon period (1951-2020) from 1470 to 2020 (Cai et al., 2001; Zhao, 2011).

**Table 1.** Precipitation corresponding to drought and flood levels.

drought and flood level	Description	Annual Precipitation Anomaly Percentage (Feasible range) (%)	Annual Precipitation(mm)
1 (Flooding)	Precipitation with long duration and high intensity, large-scale flood, and severe typhoon disasters along the coast	25 (10 ~ 30)	1439.29
2 (Partial flooding)	Continuous precipitation with less severe disasters, local flood, hurricane and heavy rain with less severe disasters in a single season	10 (5 ~ 10)	1273.22
3 (Normal)	Harvest or no record	0 (-5 ~ 5)	1107.15
4 (Partial drought)	Drought and local areas with minor disasters in a single season and	10 (-10 ~ -5)	941.07

month			
5 (Drought)	Continuous drought for several months or cross quarter drought, large-scale severe drought	-25 (-30 ~ -10)	775.00

Besides, the method for calculating the evapotranspiration is generally the same as that for the village scale, and only the part that obtains the land use/cover data is different. The LUCC before 1980 consisted mainly of transformations of cultivated land and forestland (Pan, 2021), so if the changes in cultivated land areas are compiled, the land use/cover data in the historical period can be reconstructed. In addition, the spatial distribution of LUCC is of great significance for studying the evolution of HWR, and an index called the cultivated land expansion index is constructed to reflect the sequence of cultivated land expansion. The formulas are as follows:

$$\begin{cases} CLEI = \alpha_1 NHD + \alpha_2 NRD + \alpha_3 NS \\ NHD = HD / (HD_{MAX} - HD_{MIN}) \\ NRD = RD / (RD_{MAX} - RD_{MIN}) \\ AS = \begin{cases} 0 & 0 \leq S \leq 0.25 \\ 1 & 0.25 < S \leq 1 \end{cases} \end{cases} \quad (6)$$

where  $CLEI$  is the cultivated land expansion index,  $CLEI \in [0,1]$ ; the closer  $CLEI$  is to 0, the more likely this pixel is to be developed into cultivated land earlier;  $NHD$ ,  $NRD$  and  $AS$  are the normalized habitation distance, normalized river distance and adjusted slope, respectively;  $\alpha_1$ ,  $\alpha_2$  and  $\alpha_3$  are weight coefficients,  $\alpha_1 = \alpha_2 = \alpha_3 = 1/3$ ;  $HD$ ,  $RD$  and  $S$  are the habitation distance, river distance and slope of one pixel, respectively; and  $HD_{MAX}$ ,  $HD_{MIN}$ ,  $RD_{MAX}$  and  $RD_{MIN}$  are the maximum habitation distance, minimum habitation distance, maximum river distance and minimum river distance of the whole basin, respectively, m.

### (3) Key time nodes of the evolution of HWR

Transition theory is one of the most relevant methods to understand the evolution of socioeconomic systems and support sustainable development management (Tàbara and Ilhan, 2008; Lu et al., 2015). In this research, the per capita water resources, human water consumption, forestland areas and populations are selected as indicators to understand the evolution of the HWR in the Yangchang River basin over the past 600 years. Among these indicators, the per capita water resources reflect the changes in the background conditions of water resources. Human water consumption reflects the impact of socioeconomic development on the water cycle process. The forestland area reflects the eco-environmental quality and water conservation capacity. The population reflects the degree of socioeconomic development. Finally, according to the directions and rates of change of these four indicators, the HWR can be divided into four different development stages, namely, predevelopment, take-off, acceleration and rebalancing. The formulas are as follows:

$$\begin{cases} PCWR = R/POP \\ HWC = I + DW \end{cases} \quad (7)$$

where  $PCWR$  is the per capita water resources,  $m^3$  per capital;  $POP$  is the population; and  $HWC$  is the total human water consumption,  $m^3$ .

#### (4) Data collection and processing

Three types of data are collected and used to analyse the evolution of HWR (Table 2). The first category is land use/cover data. At the village scale, the historical land use/cover data are determined by using the restored map of “Baojia Tun” (Zhou and Xu, 2018), and the modern land use/cover data are determined by using the 2020 global 30-m land use/cover data and unmanned aerial vehicle remote sensing images that were obtained by a DJI Mavic Air 2 drone. At the basin scale, the land use/cover data for the historical period consist of the cultivated land areas in the study area that were sorted and estimated from the relevant documents describing the agricultural development in Guizhou Province and Anshun city. From 1980-2020, the China multi-period 30-m land use/cover remote sensing monitoring dataset will be used, and the years without data will directly use the land use/cover data from the closest year. The second category consists of the data that are used to reconstruct the precipitation and evapotranspiration levels in the water cycle process. The precipitation amounts are determined by the drought and flood levels for the period from 1470 to 2000. Based on the measured precipitation data from meteorological stations from 1958 to 2000, the correlation between these data and the drought and flood levels can be established. For the precipitation data obtained from meteorological stations from 2001 to 2020, the inverse distance weight method will be used to calculate the area precipitation levels. The Moderate-resolution Imaging Spectroradiometer (MODIS) Terra Net Evapotranspiration product (MOD16A2.006) in the Google Earth Engine is processed to provide the annual average potential evapotranspiration and actual evapotranspiration levels for the Yangchang River basin. The third category consists of data that are used to analyse the evolution of HWR, which include population changes, per capita domestic water consumption levels, and irrigation quotas, which are obtained from the literature and statistical data.

**Table 2.** Data sources.

Data name	Date range	Purpose	Source
Restored map of “Baojia Tun”	The Ming dynasty	Reconstruct land use/cover at the village scale	(Zhou and Xu, 2018)
Global 30 m land use/cover data	2020		National Geomatics Center of China
Cultivated land area in historical period	1470-1980	Reconstruct land use/cover at the basin scale	(Zhang, 1998; Xue et al., 2014; Chen, 2016)
China multi period land use and land cover remote sensing monitoring dataset (CNLUCC) (30 metres)	1980, 1990, 2000, 2005,		(Xu et al., 2018)
Atlas of drought and flood distribution in China in recent 500 years	1470-2000	Reconstruct precipitation	(Institute of Meteorological Sciences, 1981; Zhang and liu, 1993; Zhang et al., China Meteorological Data Network( <a href="http://data.cma.cn">http://data.cma.cn</a> ))
Precipitation data of meteorological stations	1958-2020		
MOD16A2.006 Terra Net Evapotranspiration (500 metres)	2001-2020	Reconstruct evapotranspiration	GEE
Unmanned aerial vehicle low altitude remote sensing (<1 m)	2020		DJI Mavic Air 2

Landsat-7, Landsat-8 and Sentinel-2 Surface reflectance	2001-2020	Remote sensing hydrological	GEE
Population in historical period	1470-2000	Analyse the evolution of HWR	(Jiang, 1982; Yang, 1996; Zhang, 1998; Chen, 2016)
Statistical Bulletin of National Economic and Social	2001-2020		China Statistical Information
China City Statistical Yearbook	2001-2020		China Statistics Press
Water Resources Bulletin of Anshun City	2008-2019		Anshun Water Resources Bureau( <a href="http://swj.anshun.gov.cn/">http://swj.anshun.gov.cn/</a> )
Statistical Yearbook of Anshun City	2012-2019		Anshun Municipal Bureau of Statistics( <a href="http://www.anshun.gov.cn/zfsj">http://www.anshun.gov.cn/zfsj</a> )

## 4 Results

### 4.1 Water cycle process at the village scale over the past 600 years

Water cycle processes during the Ming Dynasty (1470-1636) and modern times (2020) at the village scale are analysed (Fig. 2). Fig. 2 shows that with continuous socioeconomic development, the population of “Baojia Tun” has increased from 529 to 2870, but the water cycle structure in “Baojia Tun” has generally remained stable. The socioeconomic development model still represents a small-scale peasant economy, and the human impacts on the water cycle process are still dominated by irrigation water; only the precipitation percentages that are accounted for by various elements in the water cycle process have changed.

For the evapotranspiration, the cumulative evapotranspiration accounted for 73.66% of precipitation during the Ming Dynasty, of which the evapotranspiration levels of forest and grassland (36.21%) and cultivated land were similar (35.64%), while the evapotranspiration level of construction land was very small (1.81%). In modern times, due to the expansion of cities and towns and cultivated land, large amounts of deforestation have occurred, and the forestland area has been reduced from 0.262 km<sup>2</sup> to 0.072 km<sup>2</sup>. As a result, the evapotranspiration levels of cultivated land and construction land have increased to 43.66% and 9.82%, respectively, the evapotranspiration level of forest and grassland has decreased sharply to 9.43%, and the total evapotranspiration has also decreased to 62.91%. Regarding the impacts of human activities on the water cycle process, the irrigation water consumption has increased from 35.90% to 43.97%, and the amount of irrigation return water has also increased from 27.42% to 33.59%. Although the proportion of domestic water consumption in precipitation is very small, its range of increase is as high as 542.55%. The last factor is runoff. Because forestland is the most important water conservation land use/cover type, the deforestation of forestland has led to runoff increases that range from 26.31% to 36.93%. Although the total runoff has increased significantly, the surface runoff will not increase significantly due to the simultaneous increase in irrigation water levels, which will lead to more surface runoff being converted into interflow or underground runoff.

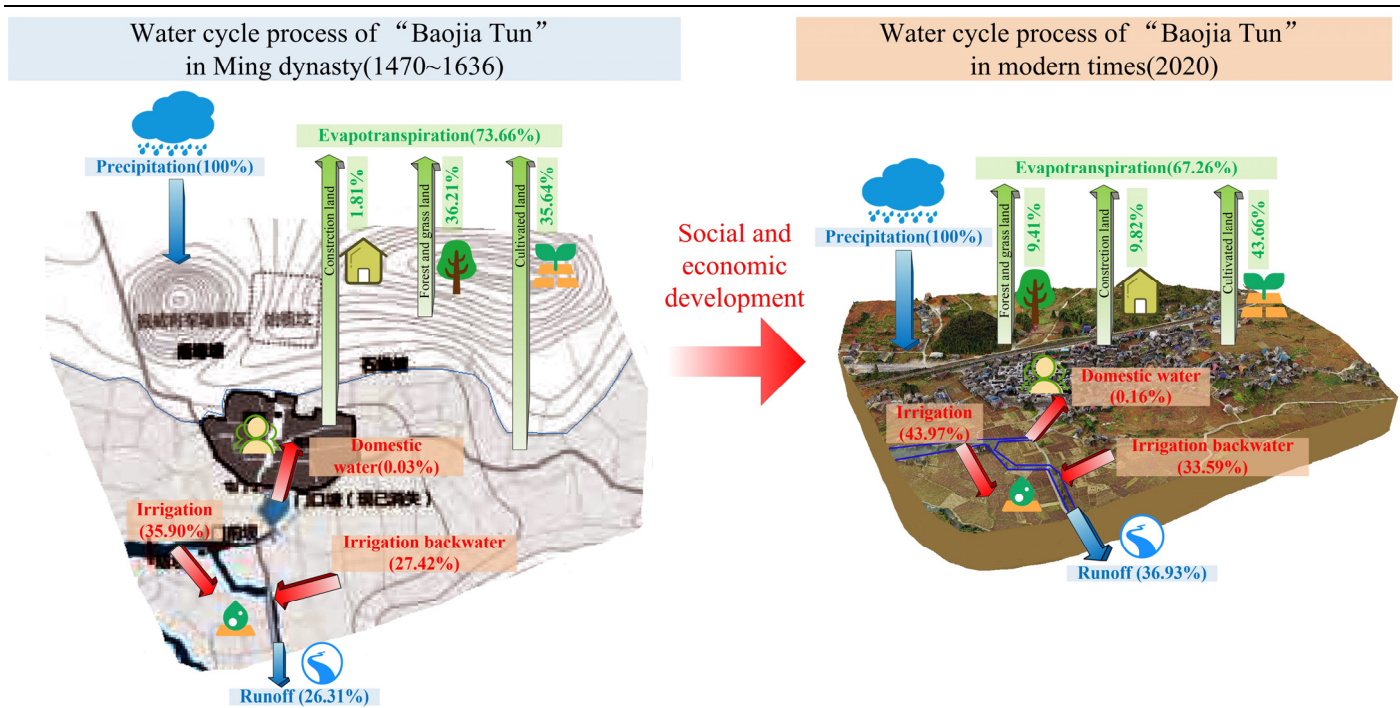


Figure 2. The change of water cycle processes in “Baojia Tun” from the Ming Dynasty to modern times.

#### 4.2 Variations in water resources at the basin scale over the past 600 years

By using correction coefficients of 0.9 and 1.1 for the precipitation during the Little Ice Age (1470-1633) and strong monsoon period (1634-1950), respectively, the precipitation, evapotranspiration and runoff time series from 1470 to 2020 are reconstructed at the basin scale (Fig. 3a). RSHS and the measured precipitation of the weather station was used to verify the accuracy of the reconstructed runoff and precipitation, respectively, the variation result of precipitation and runoff can be seen in supplementary Fig.1. Under the joint influence of precipitation and evapotranspiration, the runoff exhibited a significant increasing trend ( $P < 0.05$ ), with an average annual runoff of  $2.02 \times 10^8 \text{ m}^3$  from 1470 to 2020 and an overall rate of increase of  $8.41 \times 10^4 \text{ m}^3 \cdot \text{a}^{-1}$ . Through a further analysis of the changes in the water cycle process in different stages, it can be found that the runoff trend changed from a slow decrease to an accelerated increase, and the rate of change increased from  $-0.073 \times 10^4 \text{ m}^3 \cdot \text{a}^{-1}$  in the Ming Dynasty (1470-1636) to  $30.946 \times 10^4 \text{ m}^3 \cdot \text{a}^{-1}$  in the China stage (1949-2020) (Fig. 3b). From the Ming Dynasty to the Qing Dynasty (1636-1912), the annual average precipitation, evapotranspiration and runoff levels increased by  $0.239$ ,  $0.102$  and  $0.132 \times 10^8 \text{ m}^3$ , respectively, which indicated that the impact of human activities on the water cycle process at this stage was still slight, and the changes in various elements in the water cycle process were mainly caused by the increased precipitation. From the Qing Dynasty to the Republic of China stage (1912-1949), the change mode changed, mainly because large-scale cultivated land development occurred during this stage, and the amount of forestland greatly decreased, which thus decreased the evapotranspiration. As a result, for the condition of an annual average precipitation increase of  $0.058 \times 10^8 \text{ m}^3$ , the evapotranspiration decreased by  $0.051 \times 10^8 \text{ m}^3$  instead, which resulted in an increase in runoff of  $0.098 \times 10^8 \text{ m}^3$ . In the

---

241 Republic of China to China stage (1949-2000), for a condition of an annual average precipitation reduction of  $0.227 \times 10^8 \text{ m}^3$ ,  
242 the impact of human activities on the water cycle process remained stable but to a greater extent, which resulted in a  $0.491 \times 10^8$   
243  $\text{m}^3$  decrease in evapotranspiration and  $0.239 \times 10^8 \text{ m}^3$  increase in runoff. From the China (1949-2000) to China (2000-2020)  
244 stages, due to the joint impacts of forestland restoration and construction land expansion, the impacts of human activities on  
245 the water cycle process have changed, and the reduction in evapotranspiration that is caused by human activities has been  
246 suppressed. The annual average precipitation and evapotranspiration levels decreased by 0.009 and  $0.103 \times 10^8 \text{ m}^3$ , respectively,  
247 and the runoff increased by  $0.061 \times 10^8 \text{ m}^3$ .

248 Besides, the precipitation exhibited a periodic change trend of "decrease-increase-decrease-increase". Among them, from  
249 1470 to 1633, there was a small ice age with a dry, cold climate, and the average annual precipitation was only  $7.84 \times 10^8 \text{ m}^3$   
250 and showed a decreasing trend with a rate of  $-1.35 \times 10^4 \text{ m}^3 \cdot \text{a}^{-1}$ . From 1634 to 1949, there was a strong monsoon period with  
251 a warm, humid climate and average annual precipitation of  $8.09 \times 10^8 \text{ m}^3$ , and the precipitation during this period exhibited an  
252 increasing trend with a rate of  $3.48 \times 10^4 \text{ m}^3 \cdot \text{a}^{-1}$ . The period from 1950 to 2020 consisted of a weak monsoon period with an  
253 average annual precipitation of only  $7.90 \times 10^8 \text{ m}^3$ . Although there was a small precipitation reduction at the beginning of this  
254 period, the precipitation also exhibited an obvious increasing trend with a rate of  $16.10 \times 10^4 \text{ m}^3 \cdot \text{a}^{-1}$ , which is consistent with  
255 the increased precipitation in recent decades that is caused by climate warming.

256 In addition, the changes in evapotranspiration exhibited a trend of "increase-decrease". From 1470 to 1912, the annual  
257 average evapotranspiration was  $6.02 \times 10^8 \text{ m}^3$ , and the evapotranspiration finally exhibited an obvious increasing trend with a  
258 rate of  $3.24 \times 10^4 \text{ m}^3 \cdot \text{a}^{-1}$  due to the increased precipitation. However, the proportion of evapotranspiration for cultivated land  
259 in the total evapotranspiration gradually increased from 1.27% to 6.52% due to the increased cultivated land area (Fig. 3c).  
260 From 1913 to 2020, the average annual evapotranspiration was  $5.66 \times 10^8 \text{ m}^3$  and exhibited an obvious decreasing trend with  
261 a rate of  $-76.78 \times 10^4 \text{ m}^3 \cdot \text{a}^{-1}$ . This is because the decrease in evapotranspiration that was caused by human activities was greater  
262 than the increase in precipitation, resulting in the rapid increase in the proportion of evapotranspiration of cultivated land and  
263 construction land in the total evapotranspiration in this period, which reached maximum values of 48.48% and 1.46% in 2000-  
264 2010 and 2010-2020, respectively.

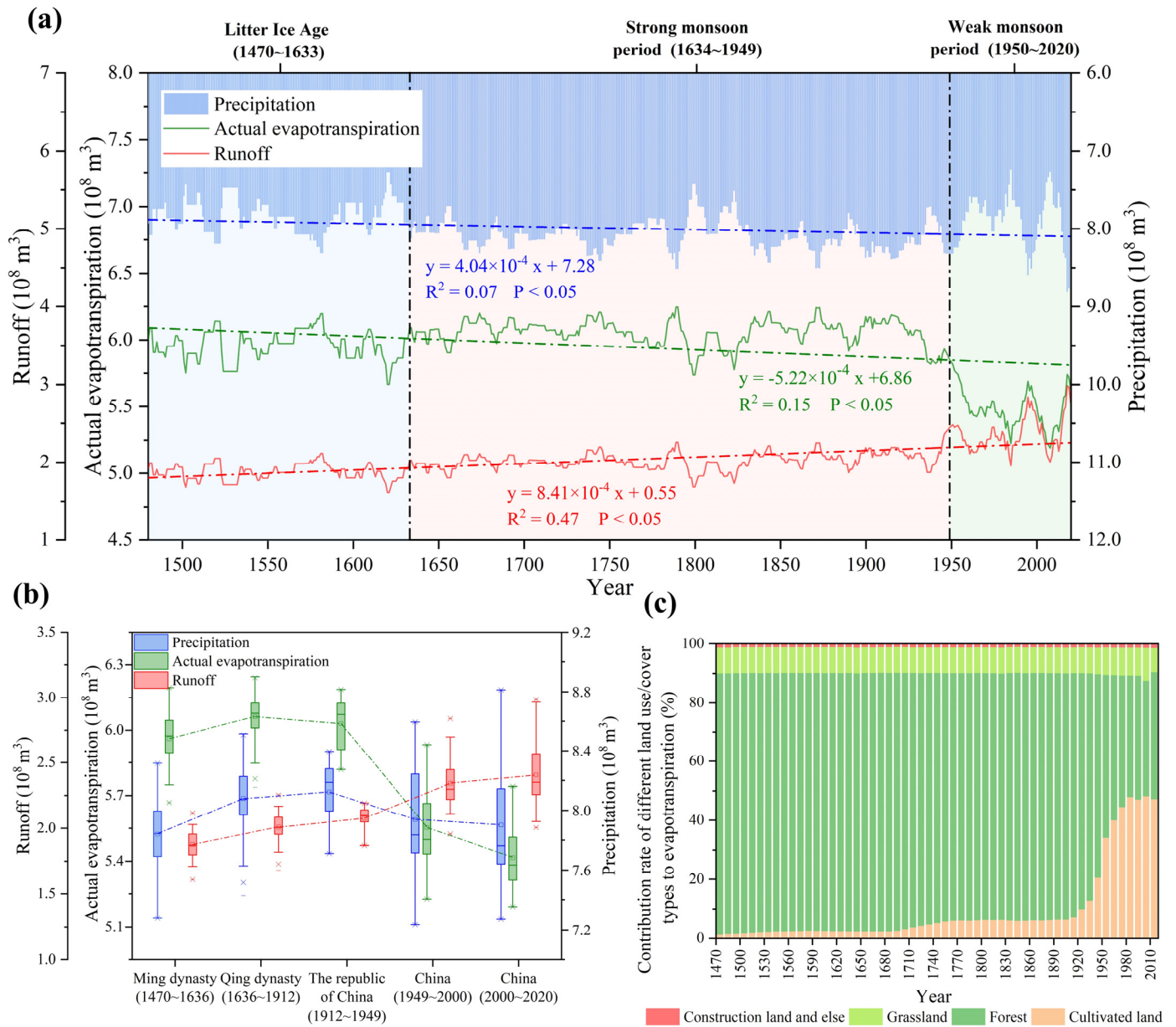


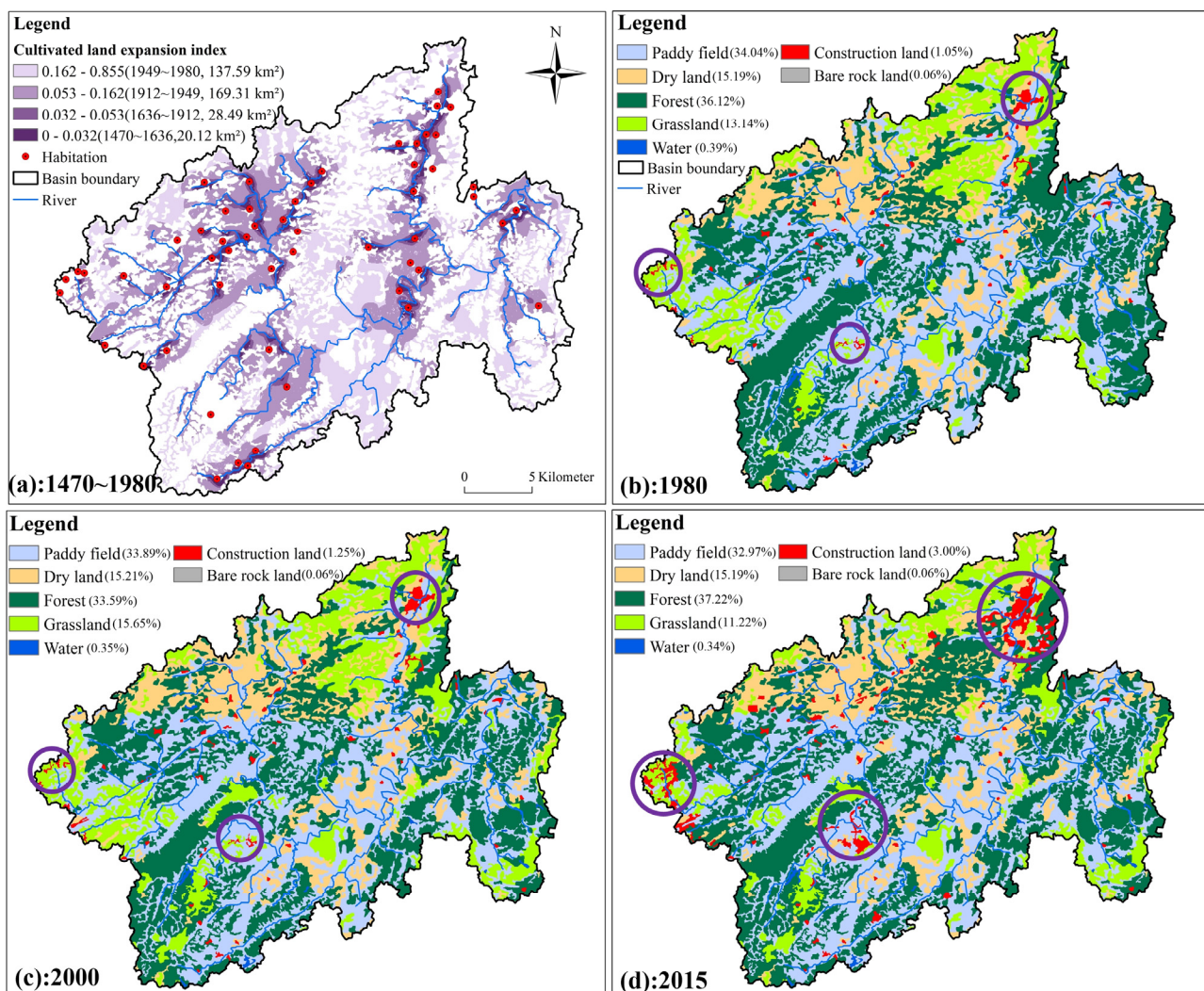
**Figure 3.** Reconstruction of the water cycle process from 1470 to 2020 at the basin scale. (a) 10-year moving average values of precipitation, evapotranspiration and runoff; (b) changes in the water cycle process in different stages; and (c) changes in composition of the cumulative actual evapotranspiration.

### 4.3 Human actions in this 600-year area

From 1470 to 1980, human activities were mainly characterised by the expansion of cultivated land, the cultivated land area was classified, and its spatial distribution was estimated (Fig. 4a). Fig. 4a shows that until 1636 (the end of the Ming Dynasty), the maximum cultivated land area was only 20.19 km<sup>2</sup>. By 1912, the end of the Qing Dynasty, the cultivated land area had increased to 49.87 km<sup>2</sup>. After that, the increase in cultivated land area entered an accelerated mode and reached

274 217.55 km<sup>2</sup> and 355.51 km<sup>2</sup> in 1949 and 1980, respectively. To reconstruct the spatial distributions of the cultivated land  
 275 expansions in the past 600 years and to divide these by periods, the cultivated land expansion index *CLEI* is calculated. The  
 276 three most appropriate thresholds were selected to cause the cultivated land area in each period to be as close as possible to  
 277 the literature results, which are 0-0.032 (20.12 km<sup>2</sup>), 0.032-0.053 (28.49 km<sup>2</sup>), 0.053-0.162 (169.31 km<sup>2</sup>) and 0.162-0.855  
 278 (137.59 km<sup>2</sup>), respectively.

279 From 1980 to 2020, six sets of 30-m land use/cover data obtained from the Chinese Academy of Sciences in 1980, 1990,  
 280 2000, 2005, 2010 and 2015 will be used directly, and the years without data will directly use the land use/cover from the  
 281 closest year (Fig. 4b-d). Fig. 4b-d shows that the LUCC from 1980 to 2020 consisted mainly of the expansion of construction  
 282 land that was supplemented by a few forestland restoration efforts. Among them, the area of construction land increased  
 283 slowly from 1980 to 2000 and showed a rapid increasing trend after 2000, from 75.95 km<sup>2</sup> in 2000 to 216.56 km<sup>2</sup> in 2015,  
 284 with an increase of 285.13%. For cultivated land, the area of dry land generally remains stable, while the area of paddy fields  
 285 continue to decrease, from 245.79 km<sup>2</sup> to 238.07 km<sup>2</sup>, a decrease of 3.14%. The total area of grassland decreased from 94.93  
 286 km<sup>2</sup> in 1980 to 81.00 km<sup>2</sup> in 2015, and the total area of forestland increased from 260.88 km<sup>2</sup> in 2000 to 268.77 km<sup>2</sup> in 2015.



287

**Figure 4.** Human actions in the past 600 years. (a) The cultivated land ranges from 1470 to 1980, (b) land use/cover in 1980, (c) land use/cover in 2000, and (d) land use/cover in 2015. The purple circles represent the areas with obvious expansions of construction land, and the circle diameters reflect the scopes of construction land.

#### 4.4 Evolution of HWR at the 600-year scale

Based on transition theory, the change slopes and average per capita values of the water resources, human water consumption, forest areas and population in the Yangchang River Basin from 1470 to 2020 are analysed. The results show that the HWR continued to develop from the initial balanced resource-rich period to an unbalanced period with extensive development and finally to a rebalancing period, which can be divided into the following four stages: predevelopment (1470-1685), take off (1685-1912), acceleration (1912-2000) and rebalancing (2000-2020) (Fig. 5).

The predevelopment stage (1470-1685) occurred from the mid-Ming Dynasty to the early Qing Dynasty. For this stage, the socioeconomic development level of the basin is slow, the water and forest resources are rich, and the overall degree of human development of water resources is low. This stage belongs to a balanced resource-rich period of HWR. In detail, the population growth is slow ( $16 \text{ people}\cdot\text{a}^{-1}$ ), and the per capita water resources exhibit a rapid decreasing trend ( $\text{Pcwr}_{k1} = -0.059 \text{ thousand m}^3$ ) under the influence of precipitation change and population growth. The short period of growth of the per capita water resources was due to the population decline from 1620 to 1637, when there were frequent wars during the change in dynasties (Sheng et al., 2019). However, the per capita water resources are relatively abundant, with an average of  $27.50 \text{ thousand m}^3\cdot(\text{capita}\cdot\text{year})^{-1}$ . Although the human water consumption showed an insignificant increasing trend ( $\text{Hwc}_{k1} = 0.0003\times 10^8 \text{ m}^3$ ), the average annual human water consumption was  $0.13\times 10^8 \text{ m}^3$ , which accounted for only 7.04% of the average runoff at this stage. At the same time, the basin was rich in forest resources, with an average forest area of  $599.93 \text{ km}^2$ , which accounted for 83% of the total basin area, and the decreasing trend is not obvious ( $\text{Fa}_{k1} = -0.92 \text{ km}^2$ ).

The take-off stage (1685-1912) occurred in the middle and late Qing Dynasty. With the decrease in warfare and gradual stabilisation of society, the level of socioeconomic development begins to increase during this stage, the human impact on the water cycle process is still slight, and the water resources and forest resources are still at relatively rich levels, but the HWR began to shift towards an imbalance. At this stage, the population began to increase ( $106 \text{ people}\cdot\text{a}^{-1}$ ). Although the decline rate of the per capita water resources was slightly lower than that of the predevelopment stage due to the increased precipitation that was caused by the strong monsoon period during this stage ( $\text{Pcwr}_{k2} = -0.041 \text{ thousand m}^3$ ), its average value was  $8.70 \text{ thousand m}^3\cdot(\text{capita}\cdot\text{year})^{-1}$ , which was only 31.65% of the value during the predevelopment stage. To meet the food needs of the increased population, the area of cultivated land expanded to a slight extent, which resulted in the increase rate of human water consumption being 300% of that of the predevelopment stage ( $\text{Hwc}_{k2} = 0.0009\times 10^8 \text{ m}^3$ ), but

---

317 its proportion of runoff is only 17.29%. Although the forest resources have decreased slightly, they are still relatively abundant.  
318 The forestland area accounts for 79.45% of the total basin area on average, but its reduction rate is 415.22% of that of the  
319 predevelopment stage ( $Fa_{k2} = -3.82 \text{ km}^2$ ).

320 The acceleration stage (1912-2000) occurred during the transition from the Republic of China to the new China. Due to  
321 the changes in the socioeconomic system and liberation of productive forces, socioeconomic development has accelerated in  
322 an extensive manner, the utilization degree of water resources has reached a high level, and the amount of water resources in  
323 the basin will have difficulty supporting higher-intensity development. Meanwhile, with the reduction in forestland, the  
324 quality of the ecological environment increasingly declined, and the HWR entered an imbalanced stage. At this stage, the  
325 population growth rate increased further ( $1711 \text{ people}\cdot\text{a}^{-1}$ ), which resulted in a faster decrease in per capita water resources  
326 ( $Pcwr_{k3} = -0.048 \text{ thousand m}^3$ ), and the average value decreased to only  $2.94 \text{ thousand m}^3\cdot(\text{capita}\cdot\text{year})^{-1}$ . Due to the surge  
327 in cultivated land irrigation and human domestic water demand, human water consumption increased rapidly ( $Hwc_{k3} =$   
328  $0.0219\times 10^8 \text{ m}^3$ ), which accounting for 61.06% of the total runoff on average, and reached a maximum value of 102.69% in  
329 1985. Meanwhile, to provide the necessary land for the expansion of cultivated land and construction land, the forestland area  
330 decreased at a very rapid rate ( $Fa_{k3} = -70.52 \text{ km}^2$ ) and reached the lowest value of  $244.47 \text{ km}^2$  in 1999.

331 The rebalancing stage (2000-2020) occurred in the China period. Due to the influence of ecological and environmental  
332 protection policies such as the ecological civilization, the basin has maintained a rapid level of socioeconomic development  
333 but also considers the protection of water resources and restoration of the ecological environment. As a result, the ecological  
334 civilization rebuilds HWR and causes them to transition to a rebalancing stage with high consumption and high output. At  
335 this stage, the population growth rate reached its highest level ( $2737 \text{ people}\cdot\text{a}^{-1}$ ). Although the average per capita value of  
336 water resources has been as low as  $1.12 \text{ thousand m}^3\cdot(\text{capita}\cdot\text{year})^{-1}$ , its decreasing trend has been alleviated to some extent  
337 ( $Pcwr_{k4} = -0.006 \text{ thousand m}^3$ ). Due to the reduced area of cultivated land, human water consumption exhibited a significant  
338 decreasing trend after increasing in the first three stages ( $Hwc_{k4} = -0.0021\times 10^8 \text{ m}^3$ ) and accounted for 83.84% of the runoff  
339 on average, which means that the Yangchang River basin relied on less water to feed more humans than before. At the same  
340 time, the forest area also exhibited an upwards trend for the first time ( $Fa_{k4} = 1.11 \text{ km}^2$ ), which also means improved eco-  
341 environmental quality and soil and water conservation capacity.

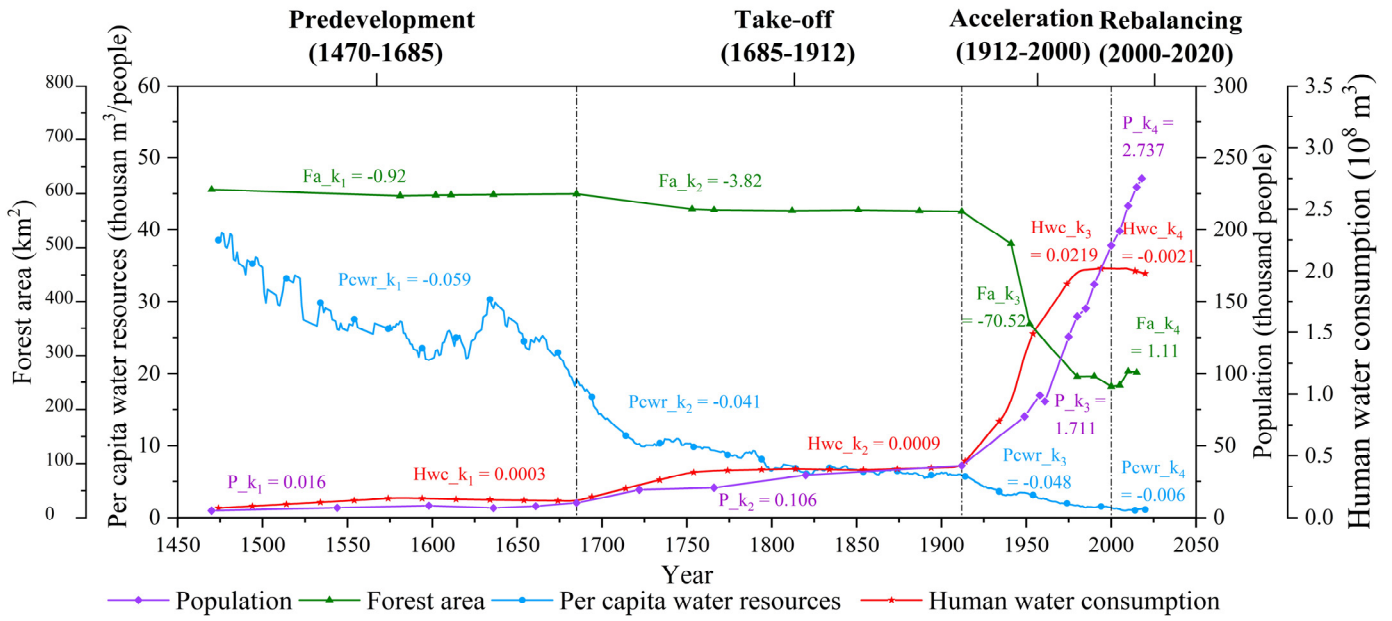


**Figure 5.** Division of the evolution stages of the HWR from 1470 to 2020. The per capita water resources and human water consumption are shown as 10-year moving averages.

## 5 Discussion

### 5.1 Why has the water cycle process remained stable at the village scale over the past six centuries?

Although the population and construction land area of “Baojia Tun” have been growing continuously over the past 600 years, the socioeconomic development mode is mainly a small-scale peasant economy, resulting in the water cycle structure remaining basically stable. Human water consumption is still dominated by irrigation water, but the percentages of the various elements in the water cycle process in the precipitation have changed (Fig. 2). From the LUCC of the whole basin, the cultivated land area in the basin has increased significantly since 1470 (the Ming Dynasty). Except for the large-scale expansion of construction land around cities and towns after 2000, the LUCC around other small residential areas are similar to those around “Baojia Tun”, so the socioeconomic development mode in the basin is still dominated by a small-scale peasant economy. Therefore, it can be inferred that the mode of human influence on the water cycle process in the basin has not changed, and the water cycle process in “Baojia Tun” can be extended to the study of the evolution of HWR at the basin scale.

The main reasons why the water cycle process in the “Tunpu” area has generally remained stable include natural factors and cultural factors. Among them, the natural factors are mainly related to the fact that the “Tunpu” area, Yangchang River basin, is located in the Anshun Plain, with open terrain, fertile soil and excellent climatic conditions. “There is seldom hot summer and cold winter”, which is suitable for the growth of crops. Therefore, the “Tunpu” area has always been an important grain production region in Guizhou Province (Chen, 2016). The specific cultural factors that are mainly present the “Tunpu”

---

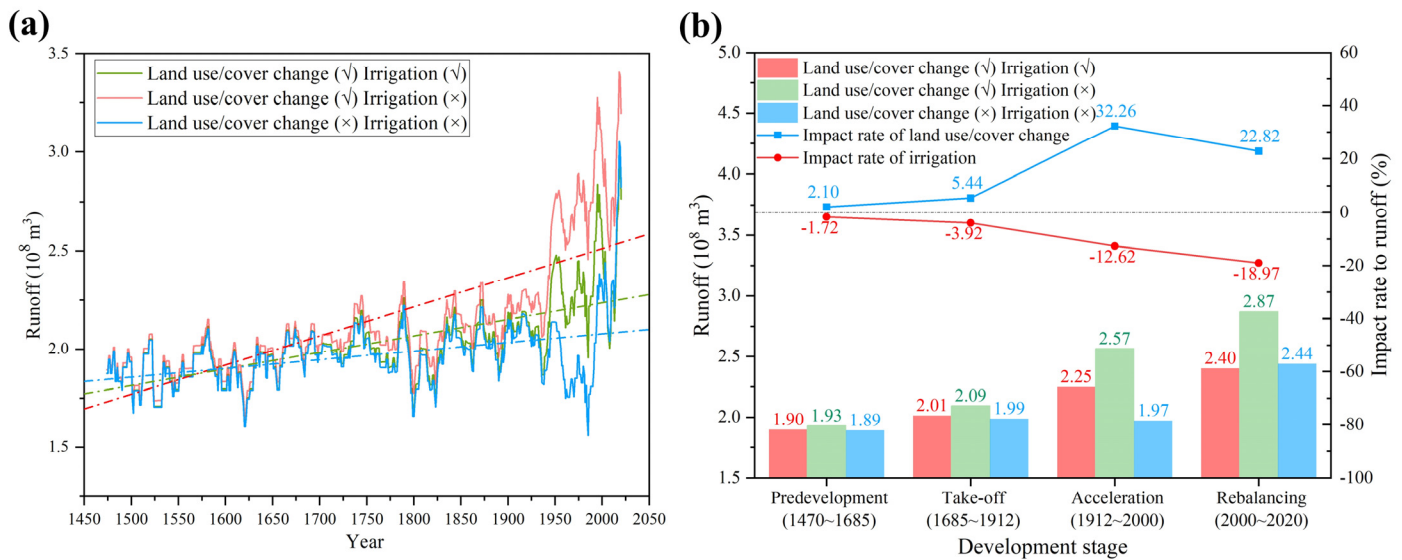
361 culture itself have academic study value and cultural value. To fully protect the “Tunpu” villages, the local government mainly  
362 focuses on the development and construction of industries such as culture and tourism by using “Tunpu” villages, which leads  
363 to the fact that the socioeconomic development mode of the entire basin is still dominated by a small-scale peasant economy,  
364 and no large-scale industrial developments have been carried out (Chen, 2018).

## 365 **5.2 What are the driving forces of the runoff changes at the basin scale?**

366 From 1470 to 2020, under the joint impacts of climate change and human activities, the runoff trend changed from a  
367 slow decrease to an accelerated increase, and the rate of change increased from  $-0.073 \times 10^4 \text{ m}^3 \cdot \text{a}^{-1}$  in the Ming Dynasty (1470-  
368 1636) to  $30.946 \times 10^4 \text{ m}^3 \cdot \text{a}^{-1}$  in the China period (e.g., 1949-2020) (Fig. 3). Regarding climate change, precipitation has the  
369 greatest impact on runoff, and there is an obvious positive correlation between precipitation and runoff ( $R^2 = 0.86$ ), which is  
370 consistent with the existing research conclusions (Yuan et al., 2019; Jiang et al., 2021). In addition, human activities can be  
371 divided into irrigation water intake and LUCC. To determine the extent of the impacts of different human activities on the  
372 water cycle process, runoff calculations under the influence of different human activities can be conducted by controlling the  
373 land use/cover or irrigation water volume (Fig. 6).

374 Fig. 6 shows that the increased runoff in the basin results from the offsetting impacts of two different human activities  
375 on the water cycle process, and the increased runoff caused by LUCC is greater than the decreased runoff caused by irrigation  
376 water intake. Under the scenario of only considering the LUCC, from 1470 to 2020, the change rate of runoff increased  
377 significantly from  $4.41 \times 10^4 \text{ m}^3 \cdot \text{a}^{-1}$  to  $14.8 \times 10^4 \text{ m}^3 \cdot \text{a}^{-1}$ . Meanwhile, the LUCC in each stage lead to runoff increases, but their  
378 impacts are different: from the predevelopment to acceleration stage, the degree of impact of the LUCC gradually increases  
379 from 2.10% to 32.26%, and the LUCC modes consist mainly of the transformation from forestland to cultivated land, which  
380 will reduce the total evapotranspiration during this period and increase the runoff (Du et al., 2018). In the rebalancing stage,  
381 the impact degree of the LUCC in the rebalancing stage is only 22.82%, and the main LUCC modes consist of the expansion  
382 of construction land and restoration of forestland, which will significantly increase the runoff levels due to the impermeability  
383 of construction land and the increased evapotranspiration of forestland (Zhao et al., 2016).

384 Then, under a scenario that considers both LUCC and irrigation at the same time, from 1470 to 2020, the change rate of  
385 runoff decreased significantly from  $14.8 \times 10^4 \text{ m}^3 \cdot \text{a}^{-1}$  to  $8.41 \times 10^4 \text{ m}^3 \cdot \text{a}^{-1}$ . It can be also found that irrigation always causes  
386 reductions in runoff, and the impact of irrigation gradually increased from -1.72% in the predevelopment stage to -18.97% in  
387 the rebalancing stage due to the continuous increase in the average cultivated land area.



388  
389 **Figure 6.** (a) Runoff under the influence of different human activities; and (b) impact rate of different human activities on the runoff.

390 **5.3 How does the policy rebuild HWR?**

391 The HWR that developed from the initial balanced resource-rich period to the unbalanced period of extensive  
 392 development finally began to transform to the rebalancing period after 2000 (Fig. 5). The reason for the rebalancing of HWR  
 393 is mainly because China recognizes that the extensive development mode is unsustainable and needs to complete the  
 394 transformation from an industrial civilization to the ecological civilization (Pan, 2012; Lu et al., 2019). In this regard, Guizhou  
 395 Province, where the “Tunpu” area is located, has responded positively and taken a series of measures. For example, in 2000,  
 396 Guizhou Province vigorously promoted an ecological construction project that focused on the Grain for Green project. In  
 397 2007, it established a strategy of "building a province with environment" and took the lead in making the strategic decision  
 398 of building the ecological civilization in China. In 2012, the construction of an important ecological security barrier in the  
 399 upper reaches of the "two rivers" will be one of the five strategic positions of Guizhou in the future. In 2016, Guizhou Province  
 400 was established as a national ecological civilization pilot area (Jiang et al., 2014). These policies are not just slogans or visions  
 401 but are real ongoing processes (Pan, 2012).

402 Taking the earliest Grain for Green project as an example, since its launch in 2000, Guizhou Province has completed the  
 403 task of the Grain for Green project of 204.72 thousand  $\text{km}^2$ , and the forest coverage rate in the entire province has increased  
 404 from 22.8% in 1975 to 59.95% in 2020. The value of the annual ecological benefit that was created by the Grain for Green  
 405 project reached 84.072 billion yuan. The soil erosion modulus decreased from 3325 tons per  $\text{km}^2 \cdot \text{a}^{-1}$  in 2000 to 631.4 tons per  
 406  $\text{km}^2 \cdot \text{a}^{-1}$  in 2017, which was 72% lower than that before the Grain for Green project (Xiao et al., 2015; Zhang & Yang, 2021).  
 407 By combining satellite remote sensing (MOD13A1.006 Terra Vegetation Indices, 500 m), aerial remote sensing and unmanned  
 408 aerial vehicle remote sensing, we can more clearly observe that the Yangchang River basin is turning green (Fig. 7). For the

---

entire basin, the average Normalized Difference Vegetation Index (NDVI) exhibited an obvious upwards trend with a rate of 0.002/year from 2001 to 2020 ( $P < 0.05$ ), which indicates that the entire basin is turning green, which is consistent with the previous land use/cover results and relevant policies. In terms of the spatial distribution, the NDVIs of 79.04% of the areas in the basin exhibit an increasing trend and are mainly distributed in the middle and south portions of the basin. The land use/cover types in these areas consist mainly of cultivated land, forest and grassland, which are the main areas for the Grain for Green project. By comparing the aerial remote sensing images and unmanned aerial vehicle remote sensing images of areas (a) and (b) shown in Fig. 8, it is clear that the conversion from sloping farmland to forestland has significantly improved the level of forestland coverage. Meanwhile, the remaining 20.96% of the areas with decreased NDVIs are mainly distributed near the large cities and towns in the basin, where the expansion of construction land was concentrated in the basin from 2001 to 2020. However, the transformation from cultivated land to forestland can still be clearly found in the images of areas (c) and (d), as shown in Fig. 8. At the same time, the low-coverage grasslands on the mountains are also changing to forestland with high coverage. This demonstrates that whether in natural areas or areas with human activities, while promoting socioeconomic development, the entire basin is also paying attention to restoring the ecological environment. The ecological civilization can rebuild HWR and cause it to gradually transition to a rebalancing stage from 2000 to 2020, which is similar to the conclusions of studies of the Tarim River Basin (Liu et al., 2014), Heihe River Basin (Lu et al., 2015) and Loess Plateau (Wu et al., 2020).

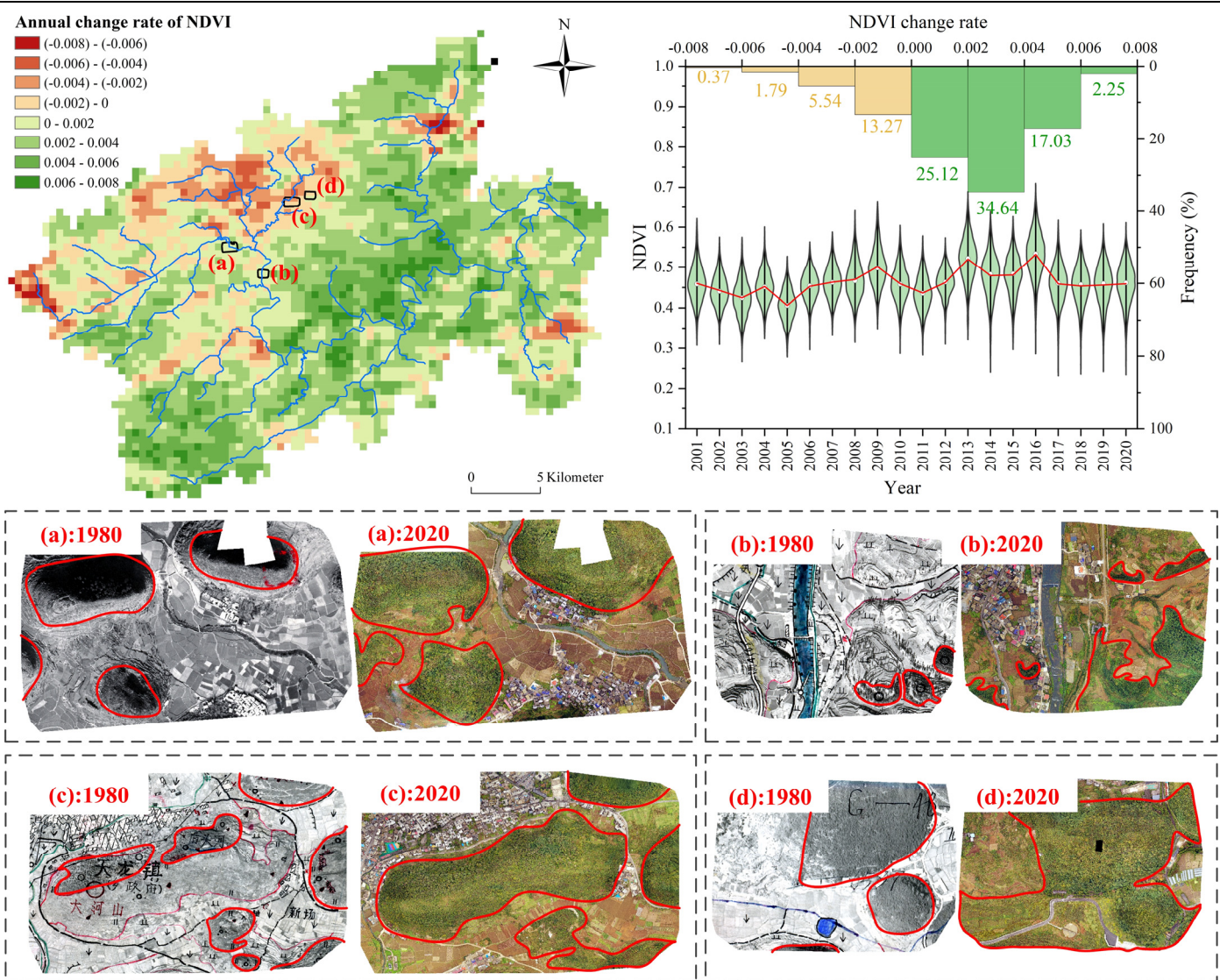


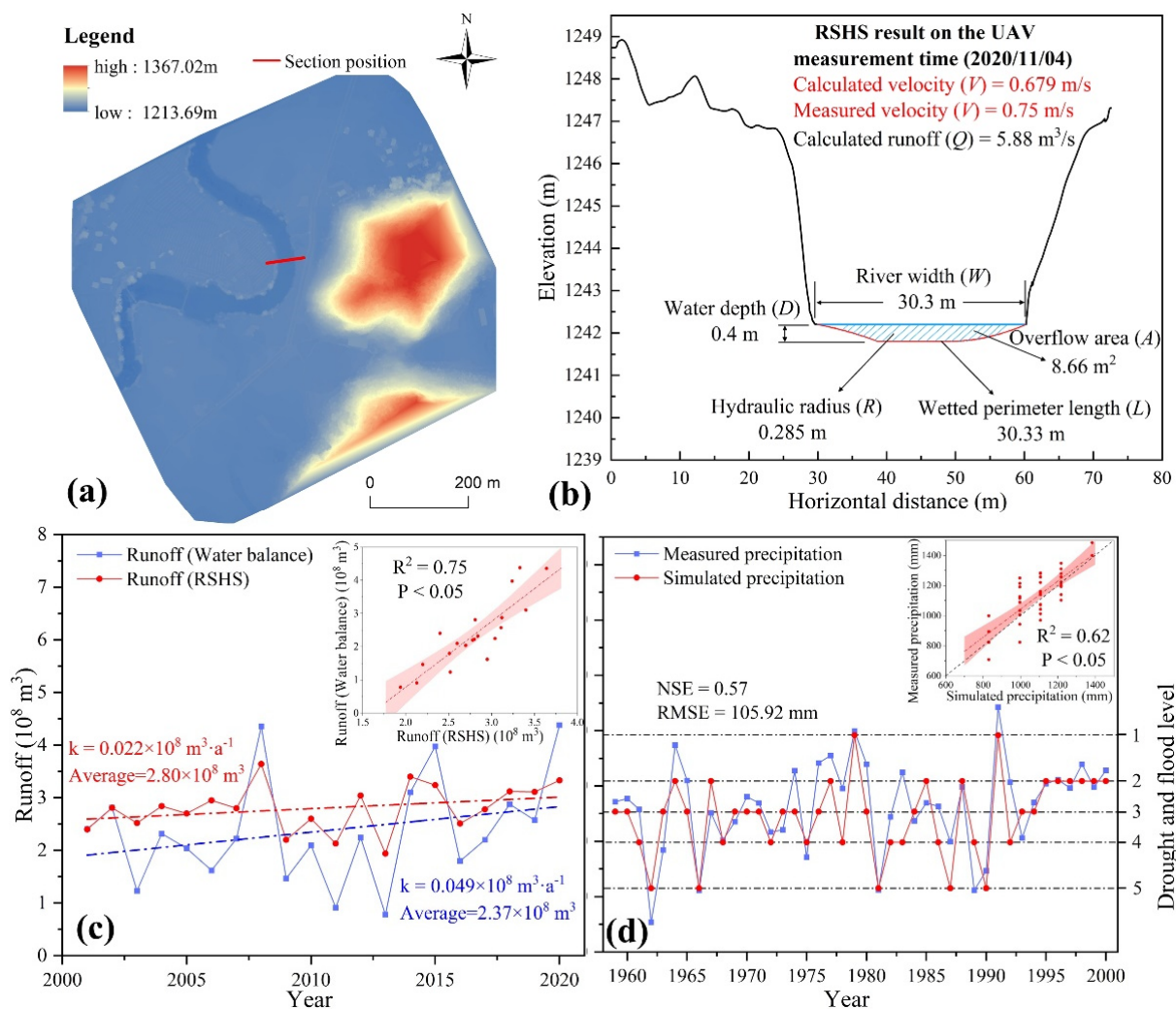
**Figure 7.** Vegetation restoration under the Grain for Green project in the rebalancing stage. The area outlined by the red line is the approximate area of vegetation growth.

#### 5.4 Validation of the method for reconstructing water cycle process over the past 600 years

The water cycle process at the basin scale in the past 600 years is reconstructed, and then the reliability analysis will be carried out from the perspective of runoff and precipitation. Firstly, based on RSHS and multi-source remote sensing data (Landsat-7, Landsat-8, Sentinel-1, Sentinel-2), the digital river model was constructed (Fig.8a and 8b) and the surface runoff from 2001 to 2020 was calculated, and then compared with the reconstructed runoff from 2001 to 2020 (Fig.8c). It can be found in Fig.6a-c that the accuracy of surface runoff estimated by RSHS is reliable. The multi-year average runoff calculated by RSHS and water balance formula is relatively close, which are  $2.80$  and  $2.37 \times 10^8 \text{ m}^3$ , respectively. Besides, through the correlation analysis chart, it can be found that there is an obvious positive correlation between the two ( $R^2 = 0.61$ ,  $P < 0.05$ ), indicating that the flow calculated by the water balance formula has the same change trend as the surface runoff calculated by

437 RSHS, which can reflect the change trend of water resources in the basin to a certain extent. Nevertheless, the total runoff  
 438 calculated by the water balance formula fluctuates greatly and is sometimes less than the surface runoff calculated by RSHS.  
 439 This is mainly because the water balance formula ignores the interannual water storage change of the basin by setting the  
 440 water storage variables of the basin to 0 for every year.

441 Then, by comparing the measured precipitation and the precipitation simulated by the drought and flood level distribution  
 442 map in *Atlas of drought and flood distribution in China in recent 500 years* from 1959 to 2000 (Fig.8d), it can be found that  
 443 there is a good positive correlation between them, and the Nash efficiency coefficient reaches 0.57. Meanwhile, in the graph  
 444 of correlation analysis, all points are distributed around the 1:1 line, the slope of linear fitting is 0.93, and  $R^2 = 0.62$ . This  
 445 shows that using the drought and flood levels in the atlas to simulate the precipitation in historical periods is reliable, and the  
 446 precipitation corresponding to each drought and flood level is set reasonably.



447  
 448 **Figure 8.** Reliability analysis of runoff and precipitation. (a) Digital Surface Model and section position; (b) river cross section elevation and  
 449 hydraulic parameter result of the UAV measurement time (2020/11/04); (c) comparison between surface runoff calculated by RSHS and the  
 450 runoff calculated by the water balance formula; and (d) comparison between measured precipitation and simulated precipitation.

---

## 6 Conclusion

By combining the historical literature, statistical data and multisource remote sensing data and taking the “Tunpu” area, Yangchang River Basin with a 600-year history of water resource development in Guizhou, China, as a typical study area, this research analyses the evolution of the HWR in different space and time spans over the past 600 years based on the RSHS technology and an improved water balance formula. Then, based on transition theory, the key time nodes in the evolution of HWR are determined, and the impacts of the ecological civilization on the HWR are analysed. The main conclusions are as follows:

At the village scale, the water cycle structure of the typical villages remained mostly stable from the Ming Dynasty to modern times, and the deforestation that was caused by the expansion of towns and cultivated land increased the proportion of runoff in precipitation by 10.62%. At the basin scale, the runoff trend changed from a slow decrease to an accelerated increase from 1470 to 2020, and the change rate increased from  $-0.073 \times 10^4 \text{ m}^3 \cdot \text{a}^{-1}$  in the Ming Dynasty (1470-1636) and gradually increased to  $30.946 \times 10^4 \text{ m}^3 \cdot \text{a}^{-1}$  in the China stage (e.g., 1949-2020), which was due to the LUCC transformations from cultivated land expansion to construction land expansion and forestland restoration, as well as the impact of fluctuating precipitation increases. The HWR have developed from the balanced initial resource-rich period to the unbalanced period of extensive development, and have finally transformed into a rebalancing period under the influence of the ecological civilization policy. The four stages are as follows: predevelopment (1470-1685), take off (1685-1912), acceleration (1912-2000) and rebalancing (2000-2020).

This research indicates that the ecological civilization policy can rebuild HWR and cause a transition to the rebalancing stage, and this policy is expected to provide enlightenment for future water resource management efforts and for the construction of the ecological civilization to further achieve the harmonious development of humans and water. Also, in addition to irrigation water and domestic water, factors such as warfare, human beliefs and consciousness that are proposed in the social sciences can affect the evolution of HWR, which need to be conducted in future studies.

## References

- Ahmad, I., Waseem, M., Lei, H., et al., 2018. Harmonious level indexing for ascertaining human-water relationships. *Environmental Earth Sciences*. 77(4). <https://doi.org/10.1007/s12665-018-7296-7>
- Bao, C., & Zou, J., 2018. Analysis of spatiotemporal changes of the human-water relationship using water resources constraint intensity index in Northwest China. *Ecological Indicators*. 84, 119-129. <https://doi.org/10.1016/j.ecolind.2017.08.056>
- Cai, Y., Peng, Z., An, Z., et al., 2001. Oxygen isotope records of Holocene stalagmites in qixingdong, Guizhou and their indication of monsoon climate change. *Scientific Bulletin*.(16), 1398-1402. (in Chinese).
- Ceola, S., Montanari, A., Krueger, T., et al., 2016. Adaptation of water resources systems to changing society and environment: a statement by the International Association of Hydrological Sciences. *Hydrological Sciences Journal-Journal Des Sciences*

483 Hydrologiques. 61(16), 2803-2817. <https://doi.org/10.1080/02626667.2016.1230674>

484 Chen, J. (2016). *The development and changes of agriculture in Anshun during the Ming and Qing Dynasties*. Guizhou Normal  
485 University. (in Chinese).

486 Chen, Y., 2018. Study on the protection and inheritance of Tunpu culture in Anshun. *Theory and Contemporary*.(11), 59-61. (in  
487 Chinese).

488 Du, L. Y., Rajib, A., & Merwade, V., 2018. Large scale spatially explicit modeling of blue and green water dynamics in a temperate  
489 mid-latitude basin. *Journal of Hydrology*. 562, 84-102. <https://doi.org/10.1016/j.jhydrol.2018.02.071>

490 Falkenmark, M., 2001. The greatest water problem: The inability to link environmental security, water security and food security.  
491 *International Journal of Water Resources Development*. 17(4), 539-554. <https://doi.org/10.1080/07900620120094073>

492 Fu, B.-P., 1981. On the calculation of the evaporation from land surface. *Chinese Journal of Atmospheric Sciences*. 5, 23-31. (in  
493 Chinese).

494 Hansen, M. H., Li, H. T., & Svarverud, R., 2018. Ecological civilization: Interpreting the Chinese past, projecting the global future.  
495 *Global Environmental Change-Human and Policy Dimensions*. 53, 195-203. <https://doi.org/10.1016/j.gloenvcha.2018.09.014>

496 Institute of Meteorological Sciences, C. M. A., 1981. Atlas of drought and flood distribution in China in recent 500 years. Map  
497 publishing house.

498 Jiang, C., Wang, Z., & Huang, W., 2014. Status of Ecological Civilization Construction in Guizhou Province and Countermeasures.  
499 *China Environmental Monitoring*.(3), 13-17. <https://doi.org/10.3969/j.issn.1002-6002.2014.03.004> (in Chinese).

500 Jiang, D., 1982. Population survey of Guizhou in the early Qing Dynasty. *Guizhou Social Sciences*.(4), 50-54. (in Chinese).

501 Jiang, J. C., Lyu, L. T., Han, Y. C., et al., 2021. Effect of Climate Variability on Green and Blue Water Resources in a Temperate  
502 Monsoon Watershed, Northeastern China. *Sustainability*. 13(4), 2193. <https://doi.org/10.3390/su13042193>

503 Leitholdt, E., Zielhofer, C., Berg-Hobohm, S., et al., 2012. Fossa Carolina: The First Attempt to Bridge the Central European  
504 Watershed-A Review, New Findings, and Geoarchaeological Challenges. *Geoarchaeology-an International Journal*. 27(1), 88-104.  
505 <https://doi.org/10.1002/gea.21386>

506 Li, K., & Xu, Z. F., 2006. Overview of Dujiangyan Irrigation Scheme of ancient China with current theory. *Irrigation and Drainage*.  
507 55(3), 291-298. <https://doi.org/10.1002/ird.234>

508 Li, Y., Li, H., Li, D., et al., 2020. Construction of rural water ecological civilization index system in China. *Water Practice and*  
509 *Technology*. 15(3), 797-806. <https://doi.org/10.2166/wpt.2020.064>

510 Liu, D., Tian, F., Lin, M., et al., 2015. A conceptual socio-hydrological model of the co-evolution of humans and water: case study  
511 of the Tarim River basin, western China. *Hydrology and Earth System Sciences*. 19(2), 1035-1054. [https://doi.org/10.5194/hess-19-](https://doi.org/10.5194/hess-19-1035-2015)  
512 [1035-2015](https://doi.org/10.5194/hess-19-1035-2015)

513 Liu, H., & Wang, L., 2018. Construction of Urban Water Ecological Civilization System. *IOP Conference Series: Earth and*  
514 *Environmental Science*. 170, 032111. <https://doi.org/10.1088/1755-1315/170/3/032111>

515 Liu, Y., Tian, F., Hu, H., et al., 2014. Socio-hydrologic perspectives of the co-evolution of humans and water in the Tarim River  
516 basin, Western China: the Taiji-Tire model. *Hydrology and Earth System Sciences*. 18(4), 1289-1303. [https://doi.org/10.5194/hess-](https://doi.org/10.5194/hess-18-1289-2014)  
517 [18-1289-2014](https://doi.org/10.5194/hess-18-1289-2014)

518 Lou, H. Z., Wang, P. F., Yang, S. T., et al., 2020. Combining and comparing an Unmanned Aerial Vehicle and multiple remote  
519 sensing satellites to calculate long-term river discharge in an ungauged water source region on the Tibetan Plateau. *Remote Sensing*.  
520 12(13), 2155. <https://doi.org/10.3390/rs12132155>

521 Lu, Y., Zhang, Y., Cao, X., et al., 2019. Forty years of reform and opening up: China's progress toward a sustainable path. *Sci. Adv*.  
522 5(8), eaau9413. <https://doi.org/doi:10.1126/sciadv.aau9413>

523 Lu, Z., Wei, Y., Xiao, H., et al., 2015. Evolution of the human-water relationships in the Heihe River basin in the past 2000 years.  
524 *Hydrology and Earth System Sciences*. 19(5), 2261-2273. <https://doi.org/10.5194/hess-19-2261-2015>

525 Nie, Z., 2017. Anshun Tunbao: here, I found the Ming Dynasty. *Tong Zhou Gong Jin* (09), 72-76.  
526 <https://doi.org/10.19417/j.cnki.tzgj.2017.09.020> (in Chinese).

527 Pan, J., 2012. From Industrial Toward Ecological in China. *Science*. 336(6087), 1397-1397.  
528 <https://doi.org/doi:10.1126/science.1224009>

529 Pan, Y. (2021). *Study on the evolution of spatial form of typical Tunpu settlements in Anshun*. Guizhou Normal University. (in  
530 Chinese).

531 Ren, C., Lu, Y., & Yang, D., 2010. Drought and flood disasters and rebuilding of precipitation sequence in Heihe River Basin in the  
532 past 2000 years. *Journal of arid land resources and environment*. 24(06), 91-95. <https://doi.org/10.13448/j.cnki.jalre.2010.06.009>  
533 (in Chinese).

534 Sha, F., & Iop. (2018, Dec 07-09). *The predicament and realization path of China's eco-civilization construction*. 4th International  
535 Conference on Advances in Energy Resources and Environment Engineering (ICAEESEE), Chengdu, PEOPLES R CHINA.

536 Sheng, Y., Zeng, M., Peng, H., et al., 2019. Reconstruction and Analysis of Dry/Wet Series in Guizhou Area in 1470-1949. *Resources*  
537 *and Environment in the Yangtze Basin*. 28(6), 1354-1364. <https://doi.org/10.11870/cjlyzyyhj201906011> (in Chinese).

538 Sivapalan, M., Savenije, H. H. G., & Blöschl, G., 2012. Socio-hydrology: A new science of people and water. *Hydrological Processes*.  
539 26(8), 1270-1276. <https://doi.org/10.1002/hyp.8426>

540 Tàbara, J., & Ilhan, A., 2008. Culture as trigger for sustainability transition in the water domain: The case of the Spanish water  
541 policy and the Ebro river basin. *Regional Environmental Change*. 8(2), 59-71. <https://doi.org/10.1007/s10113-007-0043-3>

542 Tian, P., Wu, H. Q., Yang, T. T., et al., 2021. Evaluation of urban water ecological civilization: A case study of three urban  
543 agglomerations in the Yangtze River Economic Belt, China. *Ecological Indicators*. 123.  
544 <https://doi.org/10.1016/j.ecolind.2021.107351>

545 Wang, J., Wei, Y., Jiang, S., et al., 2017. Understanding the Human-Water Relationship in China during 722 BC-1911 AD from a  
546 Contradiction and Co-Evolutionary Perspective. *Water Resources Management*. 31(3), 929-943. <https://doi.org/10.1007/s11269-016-1555-8>

547

548 Wang, P. F., Yang, S. T., Wang, J., et al., 2020. Discharge estimation with hydraulic geometry using unmanned aerial vehicle and  
549 remote sensing. *Journal of Hydraulic Engineering*. 51(04), 492-504. <https://doi.org/10.13243/j.cnki.slxb.20190742> (in Chinese).

550 Wu, X. T., Wei, Y. P., Fu, B. J., et al., 2020. Evolution and effects of the social-ecological system over a millennium in China's Loess  
551 Plateau. *Sci. Adv.* 6(41). <https://doi.org/10.1126/sciadv.abc0276>

552 Wufu, A., Chen, Y., Yang, S. T., et al., 2021. Changes in Glacial Meltwater Runoff and Its Response to Climate Change in the  
553 Tianshan Region Detected Using Unmanned Aerial Vehicles (UAVs) and Satellite Remote Sensing. *Water*. 13(13), 1753.  
554 <https://doi.org/10.3390/w13131753>

555 Xiao, L. G., & Zhao, R. Q., 2017. China's new era of ecological civilization. *Science*. 358(6366), 1008-1009.  
556 <https://doi.org/10.1126/science.aar3760>

557 Xu, X., Liu, J., Zhang, S., et al., 2018. China multi period land use and land cover remote sensing monitoring data  
558 set(CNLUCC).Data registration and publishing system of resource and environmental science data center of Chinese Academy of  
559 Sciences (<http://www.resdc.cn/DOI>), DOI:10.12078/2018070201).

560 Xue, C., Xiaobin, J., Wang, J., et al., 2014. Reconstruction and change analysis of cropland data of China in recent 300 years. *Journal*  
561 *of Geography*. 69(7), 896-906. <https://doi.org/10.11821/dlxb201407002> (in Chinese).

562 Yang, B., 1996. Analysis of Guizhou population data in the early Qing Dynasty. *Chinese Population Science*.(4), 50-54. (in Chinese).

563 Yang, Q., Gao, D., Song, D., et al., 2021. Environmental regulation, pollution reduction and green innovation: The case of the  
564 Chinese Water Ecological Civilization City Pilot policy. *Economic Systems*. 45(4). <https://doi.org/10.1016/j.ecosys.2021.100911>

565 Yang, S., Wang, P., Wang, J., et al., 2021. River Flow Estimation Method Based on UAV Aerial Photogrammetry. *Journal of Remote*  
566 *Sensing*. 25(6), 1284-1293. <https://doi.org/10.11834/jrs.20209082> (in Chinese).

567 Yang, S. T., Li, C. J., Lou, H. Z., et al., 2020. Performance of an Unmanned Aerial Vehicle (UAV) in calculating the flood peak  
568 discharge of ephemeral rivers combined with the incipient motion of moving stones in arid ungauged regions. *Remote Sensing*.  
569 12(10), 1610. <https://doi.org/10.3390/rs12101610>

570 Yang, S. T., Wang, P. F., Lou, H. Z., et al., 2019. Estimating river discharges in ungauged catchments using the slope-area method  
571 and Unmanned Aerial Vehicle. *Water*. 11(11), 2361. <https://doi.org/10.3390/w11112361>

572 Yuan, Z., Xu, J. J., Meng, X. Y., et al., 2019. Impact of Climate Variability on Blue and Green Water Flows in the Erhai Lake Basin  
573 of Southwest China. *Water*. 11(3), 424. <https://doi.org/10.3390/w11030424>

574 Zhang, D., Li, X., & Liang, Y., 2003. A further supplement to the atlas of drought and flood distribution in China in recent 500 years

575 (1993-2000). *Journal of Applied Meteorology*. 14(3), 10. (in Chinese).  
576 Zhang, D., & Liu, C., 1993. Continuation of Atlas of drought and flood distribution in China in recent 500 years (1980-1992).  
577 *Meteorology*. 19(11), 5. (in Chinese).  
578 Zhang, M., Liu, Y. M., Wu, J., et al., 2018. Index system of urban resource and environment carrying capacity based on ecological  
579 civilization. *Environmental Impact Assessment Review*. 68, 90-97. <https://doi.org/10.1016/j.eiar.2017.11.002>  
580 Zhang, W., & Pang, Y., 2007. Investigation of 600 years of water use in Baotun. *China Water Resources*.(12), 51-55.  
581 <https://doi.org/10.3969/j.issn.1000-1123.2007.12.026> (in Chinese).  
582 Zhang, X., 1998. The impact of Guizhou's population development on social economy in the Ming and Qing Dynasties. *Journal of*  
583 *Guizhou Normal University (Social Sciences Edition)*.(3), 21-25. (in Chinese).  
584 Zhao, A. Z., Zhu, X. F., Liu, X. F., et al., 2016. Impacts of land use change and climate variability on green and blue water resources  
585 in the Weihe River Basin of northwest China. *Catena*. 137, 318-327. <https://doi.org/10.1016/j.catena.2015.09.018>  
586 Zhao, C., Pan, X., Yang, S., et al., 2019. Measuring streamflow with low-altitude UAV imagery. *Acta Geographica Sinica*. 74(7),  
587 1392-1408. <https://doi.org/10.11821/dlxb201907009> (in Chinese).  
588 Zhao, K. (2011). *Stalagmite laminar chronology and isotopic climate reconstruction in donggedong, Guizhou Province in recent*  
589 *1000 years*. Nanjing Normal University. (in Chinese).  
590 Zhao, W., Ding, J., Wang, Y., et al., 2020. Ecological water conveyance drives human-water system evolution in the Heihe watershed,  
591 China. *Environmental Research*. 182. <https://doi.org/10.1016/j.envres.2019.109009>  
592 Zhou, Z., & Xu, J., 2018. Study on Water Environment and Water Landscape in Tunpu Villages in Anshun, Guizhou Province.  
593 *Journal of Western Human Settlements*.(1), 101-106. <https://doi.org/10.13791/j.cnki.hsfwest.20180116> (in Chinese).  
594 Zuo, Q., Diao, Y., Hao, L., et al., 2020. Comprehensive Evaluation of the Human-Water Harmony Relationship in Countries Along  
595 the "Belt and Road". *Water Resources Management*. 34(13), 4019-4035. <https://doi.org/10.1007/s11269-020-02632-2>  
596 Zuo, Q., Li, W., Zhao, H., et al., 2021. A Harmony-Based Approach for Assessing and Regulating Human-Water Relationships: A  
597 Case Study of Henan Province in China. *Water*. 13(1). <https://doi.org/10.3390/w13010032>

## 598 **Acknowledgement**

599 The authors thank the National Natural Science Foundation of China (Grant Nos. U1812401, 41801293) and the Key  
600 Project of Philosophy and Social Sciences Planning in Guizhou Province (19GZZD07), the Open Research Fund Program of  
601 State Key Laboratory of Hydro-science and Engineering (sklhse-2021-A-04), and the Fundamental Research Funds for the  
602 Central Universities (2017NT11). We also thank the AJE group for editing the English text of a draft of this manuscript.

## 604 **Data availability statement**

605 The data that supports the findings of this study are available in the supplementary material of this article. Among them,  
606 excel files is the data in each figure, including calculated precipitation, evapotranspiration, runoff, land use/cover change  
607 statistics, etc. Remote sensing data include, land use/cover, NDVI, evapotranspiration.

## 609 **Author contribution**

610 S.Y. contributed to methodology, software, review and editing, supervision, project administration and funding acquisition.

---

611 H.L. contributed to methodology, software, writing, calculation, review and editing and supervision. Z.P. contributed to  
612 methodology, data curation, calculation, visualization, writing. C.L., J.Z., and Y.Z. contributed to data curation, validation.  
613 Y.Y., J.G., Y.L., and X.L. contributed to data provision and supervision.

614

615 **Competing interests**

616 The authors declare no competing interests.